Journal of Hydraulic Engineering. Submitted July 12, 2010; accepted June 13, 2011;
posted ahead of print June 15, 2011. doi:10.1061/(ASCE)HY.1943-7900.0000474

Coupled Surface-Subsurface Model for Simulating Drainage from Permeable Friction Course Highways

Bradley J. Eck [1], Michael E. Barrett [2], Randall J. Charbeneau [3]

Abstract

Permeable friction course (PFC) is a porous asphalt pavement placed on top of a regular impermeable roadway. Under small rainfall intensities, drainage is contained within the PFC layer; but, under higher rainfall intensities drainage occurs both within and on top of the porous pavement. A computer model—the permeable friction course drainage code (Perfcode)—is developed to study this two-dimensional

[1]Postdoctoral Fellow, Center for Research in Water Resources, The University of Texas at Austin, Austin, TX 78712; email: brad.eck@mail.utexas.edu

[2]Research Associate Professor, Center for Research in Water Resources, The University of Texas at Austin, Austin, TX 78712; email: mbarrett@mail.utexas.edu

[3]Professor of Civil Engineering, Center for Research in Water Resources, The University of Texas at Austin, Austin, TX 78712; email: charbeneau@mail.utexas.edu

Journal of Hydraulic Engineering. Submitted July 12, 2010; accepted June 13, 2011;
posted ahead of print June 15, 2011. doi:10.1061/(ASCE)HY.1943-7900.0000474

unsteady drainage process. Given a hyetograph, geometric information with regard to the roadway layout, and hydraulic properties of the PFC media, the model predicts the variation of water depth within and on top of the PFC layer through time. The porous layer is treated as an unconfined aquifer using Darcy's law and the Dupuit-Forchheimer assumptions. Surface flow is modeled using the diffusion wave approximation to the Saint-Venant equations. A mass balance approach is used to couple surface and subsurface phases. Straight and curved roadway geometries are accommodated via a curvilinear grid. The model is validated using steady state solutions that were obtained independently. Perfcode was applied to a field monitoring site near Austin, Texas and hydrographs predicted by the model were consistent with field measurements. For a sample storm studied in detail, PFC reduced the duration of sheet flow conditions by 80%. In a second sample storm, PFC prevented sheet flow conditions completely. The model may be used to improve the drainage design of PFC roadways.

Keywords: Hydraulic Models, Porous Pavement, Sheet Flow, Dupuit-Forchheimer

Introduction

Conventional highways are paved with concrete or asphalt and drainage occurs across the roadway according to the longitudinal and cross-slope. Drainage may be improved by overlaying the roadway with porous asphalt so that drainage occurs within the pavement rather than across it. The overlay of porous asphalt—called permeable friction course (PFC) or open graded

Journal of Hydraulic Engineering. Submitted July 12, 2010; accepted June 13, 2011;
posted ahead of print June 15, 2011. doi:10.1061/(ASCE)HY.1943-7900.0000474

friction course (OGFC)—is commonly placed in a 50mm or thinner layer on top of conventional, impermeable, pavement. During rain events, water seeps into the porous layer and flows to the side of the road by gravity. By removing water from the road surface, PFC improves safety by reducing splashing and hydroplaning (Berbee et al., 1999). In addition to safety benefits, PFC has also been shown to reduce pollutants commonly observed in highway runoff (Barrett, 2008).

Although usually placed in a 50mm layer, the PFC thickness may be selected so that all of the rainfall for a design event drains within the pavement. Structural and cost concerns prevent the use of an arbitrarily thick porous layer. Additionally, PFC has been shown to clog over time, resulting in lower subsurface drainage capacity (NCHRP, 2009). Therefore, some storms will exceed the installed capacity, forcing drainage to occur both on the pavement surface and within the porous matrix. This paper describes a model for this coupled unsteady drainage process.

Three authors have published predictions of water depth in PFC for straight roadway sections under constant rainfall. Ranieri (2002) gives a numerical solution to the governing equation and a design chart. Tan et al. (2004) use a commercial finite element program to model flow through PFC. Both Ranieri (2002) and Tan et al. (2004) provide charts to find the required thickness of PFC from slope information and rainfall intensity. Charbeneau and Barrett (2008) provide an analytical solution for the saturated thickness along the flow path.

These three papers consider the same roadway geometry: a straight road

Journal of Hydraulic Engineering. Submitted July 12, 2010; accepted June 13, 2011;
posted ahead of print June 15, 2011. doi:10.1061/(ASCE)HY.1943-7900.0000474

with constant longitudinal slope and cross slope. The drainage slope is the Pythagorean sum of the longitudinal slope and the cross slope. In these papers, the drainage slope is a constant, making the problem one dimensional. Under constant rainfall intensity the system reaches a steady state. It is this one-dimensional steady state solution that these authors present. A comparison of their predictions reveals that Charbeneau and Barrett (2008) and Ranieri (2002) have essentially identical results. Tan et al. obtain a different result, predicting a thinner porous layer than the other workers. The reasons for this discrepancy are difficult to uncover because Tan et al. used a commercial finite element program for analysis.

Very little has been mentioned in the literature regarding the coupling between surface and subsurface flow in PFCs. Charbeneau and Barrett (2008) address the issue briefly and provide an estimate of sheet flow thickness based on the Darcy-Weisbach equation. Eck et al. (2011) refined the coupling between PFC and sheet flow by using a different boundary condition for the PFC equation. Their idea was to compute the location that sheet flow begins based on the principle of continuity and use that location and the pavement thickness as the initial point to integrate the first order ODE that governs the PFC part of the problem.

Although unsteady PFC drainage has not been addressed directly, many hydrologic models couple surface and subsurface flow processes. Most models focus on flow in only one phase, and use the other phase as a boundary condition. For example, in an irrigation system, the detailed solution of the groundwater system is not of interest; the objective is a good representation

Journal of Hydraulic Engineering. Submitted July 12, 2010; accepted June 13, 2011;
posted ahead of print June 15, 2011. doi:10.1061/(ASCE)HY.1943-7900.0000474

of surface flow and infiltration. In the same way, subsurface flow models such as MODFLOW focus on the solution to the groundwater system, which is usually unaffected by the sheet flow dynamics. In contrast, models of entire watersheds do attempt to represent surface flow, infiltration, and subsurface flow. However, a detailed solution for overland flow is rarely found along with a detailed groundwater solution. Two notable exceptions are the work of He et al. (2008) and the MIKE SHE model.

He et al. (2008) present a "Coupled Finite-Volume Model for 2D Surface and 3D Subsurface Flows." This model couples a diffusion wave model on the surface with Richards equation in the subsurface. The coupling is accomplished by requiring the pressure to be continuous at the land surface. This formulation treats overland flow as a boundary to subsurface flow. The model predicts the variation of surface water depth through time over the watershed.

The MIKE-SHE model, maintained by the Danish Hydrologic Institute, Inc, is a commercial software package for watershed simulation. The model simulates the major hydrological processes that occur in the land phase of the hydrologic cycle, including surface flow and groundwater flow (Refsgaard and Storm, 1995). For coupling between surface and subsurface phases, the program calculates the exchange flux from Darcy's law. The MIKE-SHE model has been used widely to model many watersheds and is often used to evaluate new models (e.g. He et al., 2008).

Other models that couple surface and subsurface processes have been reviewed by Furman (2008). In his review, Furman categorizes models ac-

Journal of Hydraulic Engineering. Submitted July 12, 2010; accepted June 13, 2011;
posted ahead of print June 15, 2011. doi:10.1061/(ASCE)HY.1943-7900.0000474

cording to the type of surface flow and subsurface flow that the model uses. In his summary of 26 models, there are seven models that deal with surface flow in two dimensions—of these only one deals with the subsurface as a groundwater problem instead of infiltration or partial saturation. The one model that does both is a unique application by Liang et al. (2007) where buildings in the floodplain are modeled as a porous medium. In their formulation, Liang et al. (2007) restrict the solution at any point in the system to either surface flow or subsurface flow. The coupling is horizontal; water from the flood wave flows laterally into the buildings.

The research described in the present paper shares many attributes with previous studies–predicting water depth and runoff from rainfall is a hydrologic model. The original contribution of this work comes from several areas:

- The model predicts the transient response of PFC, which has yet to be addressed in the literature.
- In the PFC system, subsurface flow drives overland flow. This forcing contrasts with the natural process of ponding from overland flow causing infiltration.
- A new boundary condition is developed for PFC highways.

The following theoretical development may be inaccessible to some practitioners. Our primary goal is to establish the theoretical basis for modeling unsteady drainage from PFC highways so that the resulting model can be applied to cases of practical interest such as complex roadway geometry.

Journal of Hydraulic Engineering. Submitted July 12, 2010; accepted June 13, 2011;
posted ahead of print June 15, 2011. doi:10.1061/(ASCE)HY.1943-7900.0000474

Mathematical Model

The processes represented in this model are precipitation, saturated porous media flow, and overland flow. Infiltration and partially saturated porous media flow are neglected because the hydraulic conductivity of the porous layer is much greater than the rainfall rate. Precipitation is assumed to be a known function of time. Flow within and on top of the PFC layer is modeled using the partial differential equations (PDEs) given in this section.

Figure 1 is a sketch of the dimensional variables used to represent different physical quantities. The rainfall rate $r(t)$ is assumed to be spatially uniform, but variable in time. The elevation of the bottom of the PFC layer with respect to a datum is $z(x, y)$. The PFC layer has a thickness b, which is taken as constant throughout the domain. The saturated thickness of water in the PFC layer is $h_p(x, y)$ where the subscript refers to the pavement. The specific discharge through the PFC is $\vec{q}$. On the pavement surface, the thickness of sheet flow is $h_s(x, y)$ and the average velocity is $\vec{v}$. The total head of water at any point in the domain is $H(x, y)$. The elevation, flow depths, and total head are related through

$$H = z + h_p + h_s \tag{1}$$

The PFC is treated as an unconfined aquifer of variable saturated thickness using Darcy's law and the Dupuit-Forchheimer assumptions. The governing equation for unsteady flow is then the Boussinesq equation (Halek and

Journal of Hydraulic Engineering. Submitted July 12, 2010; accepted June 13, 2011;
posted ahead of print June 15, 2011. doi:10.1061/(ASCE)HY.1943-7900.0000474

Svec, 1979), which may be written

$$n_e \frac{\partial h_p}{\partial t} = \nabla \cdot (K h_p \nabla H) + r \tag{2}$$

In Eq. 2 the porous medium is characterized by the effective porosity n_e and the saturated hydraulic conductivity K. The equation is non-linear because the PFC saturation thickness h_p multiplies the hydraulic gradient.

Building on the work of Jeong and Charbeneau (2010), the diffusion wave approximation to the Saint-Venant equations is used to model sheet flow. Their formulation uses a vectorized form of Mannings equation because of its simplicity and because it gives good agreement with experimental measurements (see also Charbeneau et al., 2009).

$$\frac{\partial h_s}{\partial t} = \nabla \cdot (D(h_s) \nabla H) + r \tag{3}$$

where the diffusion coefficient is related to the Manning coefficient n and friction slope S_f through

$$D(h_s) = \frac{1}{n} \frac{h_s^{5/3}}{\sqrt{S_f}} \tag{4}$$

The governing Eqs. 2 and 3 can be added to form a single equation, though only one rainfall term is included

$$n_e \frac{\partial h_p}{\partial t} + \frac{\partial h_s}{\partial t} = \nabla \cdot (K h_p \nabla H) + \nabla \cdot (D(h_s) \nabla H) + r \tag{5}$$

The time derivatives in Eq. 5 reflect the two distinct flow regimes of this system. In regime 1, the flow is contained completely within the pavement and the total head changes as the PFC saturated thickness. In regime 2,

Journal of Hydraulic Engineering. Submitted July 12, 2010; accepted June 13, 2011;
posted ahead of print June 15, 2011. doi:10.1061/(ASCE)HY.1943-7900.0000474

the PFC is full and the total head changes through the sheet flow thickness. Since $\partial z/\partial t = 0$ the regimes are summarized mathematically as

$$\frac{\partial H}{\partial t} = \begin{cases} \frac{\partial h_p}{\partial t} & for\ h_p < b \\ \frac{\partial h_s}{\partial t} & for\ h_p \geq b \end{cases} \tag{6}$$

The difference between these flow regimes is the PFC porosity, which plays a role only when the PFC is not full. A porosity function is defined to apply the porosity to the equation based on the flow condition.

$$pf = \begin{cases} 1\ for\ H - z \geq b \\ 1/n_e\ for\ H - z < b \end{cases} \tag{7}$$

With the time derivatives expressed in a single variable, we turn now to the spatial derivatives and consider the physical constraints on the flow thicknesses. The PFC saturated thickness must be positive and no greater than the pavement thickness; and the sheet flow thickness must be positive.

$$\begin{gathered} 0 \leq h_p \leq b \\ h_s \geq 0 \end{gathered} \tag{8}$$

These constraints can be expressed in terms of minimum and maximum functions for the depths, thereby eliminating them from the governing equation.

$$\begin{gathered} h_p = min(b; H - z) \\ h_s = max(0; H - z - b) \end{gathered} \tag{9}$$

Use of these functions means that the overall equation is no longer smooth in the mathematical sense; however the physical system under consideration is not smooth either. There is a shift in the behavior of the system when

Journal of Hydraulic Engineering. Submitted July 12, 2010; accepted June 13, 2011;
posted ahead of print June 15, 2011. doi:10.1061/(ASCE)HY.1943-7900.0000474

the PFC layer becomes saturated and sheet flow begins, or when sheet flow disappears into the pavement because the rainfall intensity decreased. The minimum and maximum functions have the advantages of ease of implementation in a numerical scheme and of facilitating the use of a single equation to describe subsurface flow and combined surface/subsurface flow. Using Eqs. 6, 7 and 9, governing Eq. 5 can be re-expressed using the total head as the dependent variable

$$\frac{\partial H}{\partial t} = pf * \nabla \cdot [K min(b; H - z) \nabla H] + pf * \nabla \cdot [D(max(0; H - z - b)) \nabla H] + pf * r \tag{10}$$

When the saturated thickness h_p is less than the thickness of the PFC layer, the porosity function is active, the max function removes the sheet flow term, and Eq. 10 reduces to the Boussinesq equation. When the saturated thickness is equal to or greater than the thickness of the PFC layer, the porosity function turns off, the minimum function forces the saturated thickness to the PFC layer thickness, and the surface flow term is active.

The forgoing development made simplifying assumptions about the physical system. In the subsurface it was assumed that pressure varies hydrostatically (Dupuit-Forchheimer) and that porous media flow is slow enough to neglect inertial effects (Darcy's law). The validity of Darcy's law may be checked for a specific model application by computing a porous media Reynolds number

$$Re = \frac{q\, d}{\nu} \tag{11}$$

where q is the specific discharge, d is the mean grain diameter of the porous

Journal of Hydraulic Engineering. Submitted July 12, 2010; accepted June 13, 2011;
posted ahead of print June 15, 2011. doi:10.1061/(ASCE)HY.1943-7900.0000474

media, and ν is the kinematic viscosity of the fluid. According to Bear (1972), Darcy's law is valid for Re less than some value between 1 and 10. In applying Darcy's law the PFC is assumed isotropic so a single value of the hydraulic conductivity is used. For the overland flow part of the problem, the simplifying assumption is the diffusion wave approximation to the Saint-Venant equations. The diffusion wave model is appropriate for urban slopes (Daluz-Vieira, 1983) and there is a precedent for its use set by Jeong and Charbeneau (2010).

Computational Grid

The model developed here uses the same computational grid developed by Joeng and Charbeneau (2010). Briefly, each point along the roadway centerline is assumed to lie on the circumference of a circle. The coordinates of the center of the circle may be given explicitly, or estimated from neighboring points. The radius of curvature is assumed to vary linearly along the centerline between known points. This scheme accommodates straight roadways through a large radius of curvature. A sample grid between two roadway centerline points is shown in Figure 2. The grid is curvilinear in physical x, y coordinates but becomes rectangular when transformed to ξ, η space.

The coordinates of each known point on the centerline and its corresponding center of curvature are used to map the curvilinear roadway to a rectangular representation using the transformation functions (Jeong and

Journal of Hydraulic Engineering. Submitted July 12, 2010; accepted June 13, 2011;
posted ahead of print June 15, 2011. doi:10.1061/(ASCE)HY.1943-7900.0000474

Charbeneau, 2010)

$$x(\xi,\eta) = x_{cc1} + \xi\,\Delta x + [R_1 + \xi\,\Delta R + (\eta - 0.5)W]\cos(\Theta_1 + \xi\,\Delta\Theta)$$
$$y(\xi,\eta) = y_{cc1} + \xi\,\Delta y + [R_1 + \xi\,\Delta R + (\eta - 0.5)W]\sin(\Theta_1 + \xi\,\Delta\Theta) \tag{12}$$

The length ℓ, and width ω of a line segment centered at the point (ξ,η) are computed using the partial derivatives of the coordinate transformation functions:

$$\ell(\xi,\eta) = \Delta\xi\sqrt{(\tfrac{\partial x}{\partial \xi})^2 + (\tfrac{\partial y}{\partial \xi})^2}$$
$$\omega(\xi,\eta) = W\Delta\eta \tag{13}$$

with $\Delta\xi = 1/N_\xi$ and $\Delta\eta = 1/N_\eta$, N being the number of elements in each direction.

Numerical Formulation

The finite volume method (FVM) is used to develop a numerical model of Eq. 10. The FVM is applied by integrating the governing equation over a grid cell, dividing by the cell area, ΔA , and applying the divergence theorem to the diffusive terms to give

$$\frac{\partial H_{i,j}}{\partial t} = \frac{pf}{\Delta A}\int_\Gamma K h_p \nabla H \cdot \hat{n}\; d\Gamma + \frac{pf}{\Delta A}\int_\Gamma D(h_s)\nabla H \cdot \hat{n}\; d\Gamma + pf * r \tag{14}$$

Since the divergence theorem facilitates the summing of fluxes around a grid cell, the FVM is equivalent to constructing a mass balance for each grid cell. This is a useful concept because flux components can be formulated individually for PFC flow and sheet flow.

Journal of Hydraulic Engineering. Submitted July 12, 2010; accepted June 13, 2011;
posted ahead of print June 15, 2011. doi:10.1061/(ASCE)HY.1943-7900.0000474

The integrals in Eq. 14 are the flow rates due to surface and subsurface flow. The integrals are evaluated counterclockwise around the cell boundary Γ to give the sign convention that flow into a grid cell is positive. In this way the model equation may be written

$$\frac{\partial H_{i,j}}{\partial t} = \frac{pf}{\Delta A}(Q_{p,w}+Q_{s,w}+Q_{p,e}+Q_{s,e}+Q_{p,s}+Q_{s,s}+Q_{p,n}+Q_{s,n})+pf*r \quad (15)$$

where the first subscript on the volumetric flow rate indicates flow in the pavement or on the surface and the second subscript refers to the grid cell face by compass direction. For example, $Q_{s,w}$ is the flow rate on the surface through the western face of the grid cell.

Subsurface flow rates are computed using Darcy's law with a central difference approximation for the hydraulic gradient. The flow rate is evaluated at the midpoint of each face. The formula for the western face is given here; other faces are computed analogously.

$$Q_{p,w} = K\frac{H_{i-1,j} - H_{i,j}}{1/2(\ell_{i-1,j} + \ell_{i,j})}h_{p,w}\omega_{i,j} \quad (16)$$

The variables ℓ and ω refer to the length and width of a grid cell at the cell center. The lengths and widths are evaluated using Eq. 13. Note that using the metric coefficients corresponding to each cell face is equivalent to using the actual lengths and widths.

A similar approach is used for sheet flow: the flow rate for surface flow is computed using the velocity estimate from Mannings equation and a central difference is used to estimate the hydraulic gradient. The formula for the

Journal of Hydraulic Engineering. Submitted July 12, 2010; accepted June 13, 2011;
posted ahead of print June 15, 2011. doi:10.1061/(ASCE)HY.1943-7900.0000474

western face is

$$Q_{s,w} = \frac{1}{n}\frac{h_{s,w}^{2/3}}{S_{f,w}}\frac{H_{i-1,j} - H_{i,j}}{1/2(\ell_{i-1,j} + \ell_{i,j})}h_{s,w}\omega_{i,j} \tag{17}$$

The friction slope terms are estimated using a weighted average method. The ξ component of the friction slope at the middle of the west face is computed from the node values of neighboring cells.

$$S_{f\xi,w} = \frac{H_{i-1,j} - H_{i,j}}{1/2(\ell_{i-1,j} + \ell_{i,j})} \tag{18}$$

The η component at the western face is estimated as the weighted average of the η component at the north and south faces of the central cell and its western neighbor.

$$S_{f\eta,w} = \frac{(S_{f\eta,n} + S_{f\eta,s})\ell_{i-1,j} + (S_{f\eta,n} + S_{f\eta,s})_{i-1}\ell_{i,j}}{2(\ell_{i,j} + \ell_{i-1,j})} \tag{19}$$

The magnitude of the total friction slope at any location is the Pythagorean sum of the components.

$$S_{f,w} = \sqrt{{S_{f\xi,w}}^2 + {S_{f\eta,w}}^2} \tag{20}$$

To estimate h_p and h_s in Eqs. 16 and 17, the minimum and maximum functions of Eq. 9 are combined with a linearly interpolated estimate of the total head at the cell boundary.

$$\begin{aligned} h_{p,w} &= min(b; \tfrac{H_{i,j}\ell_{i-1,j} + H_{i-1,j}\ell_{i,j}}{\ell_{i,j} + \ell_{i-1,j}} - z_w) \\ h_{s,w} &= max(0; \tfrac{H_{i,j}\ell_{i-1,j} + H_{i-1,j}\ell_{i,j}}{\ell_{i,j} + \ell_{i-1,j}} - z_w - b) \end{aligned} \tag{21}$$

The head difference (e.g. $H_{i-1,j} - H_{i,j}$) may be factored from the surface and subsurface flow rates, leaving the remaining values as a conveyance

Journal of Hydraulic Engineering. Submitted July 12, 2010; accepted June 13, 2011;
posted ahead of print June 15, 2011. doi:10.1061/(ASCE)HY.1943-7900.0000474

coefficient for each face.

$$C_w = \left(\begin{array}{l} K * min(b; \frac{H_{i,j}\ell_{i-1,j}+H_{i-1,j}\ell_{i,j}}{\ell_{i,j}+\ell_{i-1,j}} - z_w) \\ +\frac{1}{n}\frac{max(0; \frac{H_{i,j}\ell_{i-1,j}+H_{i-1,j}\ell_{i,j}}{\ell_{i,j}+\ell_{i-1,j}} - z_w - b)^{5/3}}{\sqrt{S_{f,w}}} \end{array} \right) \left(\frac{2\omega_{i,j}}{\ell_{i-1,j} + \ell_{i,j}} \right) \left(\frac{1}{\Delta A} \right) \quad (22)$$

The conveyance coefficients may be used to write the overall model equation as

$$\frac{\partial H_{i,j}}{\partial t} = pf*[C_w H_{i-1,j} + C_s H_{i,j-1} - (C_w + C_s + C_n + C_e) H_{i,j} + C_n H_{i,j+1} + C_e H_{i+1,j} + r] \quad (23)$$

Eq. 23 applies to each grid cell in the domain and therefore represents a system of equations. The equations are non-linear because the conveyance coefficients are a function of the total head.

The development given here has used the total head as the dependant variable to keep the equations as simple as possible. The model implementation uses the total thickness ($h = h_p + h_s = H - z$) as the dependant variable because the roadway elevation is normally much larger than the flow thickness. The Crank-Nicolson method (Ferziger and Peric, 2002) is used to solve final system equations. Within each timestep the system is linearized using Picard iteration. Within each iteration the penta-diagonal linear system is solved using the Gauss-Seidel method.

Journal of Hydraulic Engineering. Submitted July 12, 2010; accepted June 13, 2011;
posted ahead of print June 15, 2011. doi:10.1061/(ASCE)HY.1943-7900.0000474

Boundary Conditions

Kinematic Boundary Conditions for PFC Flow

Formulating boundary conditions for PFC flow–especially under unsteady conditions–is difficult because the solution at the boundary varies according to the external forcing (rainfall), the solution within the domain, and the geometry of the domain itself. In addition, the boundary condition should be able to transition back and forth between sheet flow and purely subsurface flow conditions.

Strictly speaking, the edge of a PFC is a seepage face because the pressure at any point along the edge is atmospheric. Treating the edge of pavement as a seepage surface is problematic for at least two reasons: (1) the velocity field near a seepage face has a strong vertical component (see the experiments of Simpson et al. 2003) but the model equation excludes vertical velocities; and (2) the Dupuit-Forchheimer assumptions on which the model is based do not allow for a seepage surface since they require the pressure to vary along a vertical line.

To overcome these challenges it is desirable to specify the saturated thickness at the center of a boundary grid cell based on the forcing, geometry, and solution from the previous time step. The center of a boundary cell is a nodal unknown, the value of which is referred to by the adjacent cells. Specifying the value at such a location is a Dirichlet condition because the value of the solution is prescribed. The following formulation develops a new method for specifying boundary conditions to a Dupuit-Forchheimer flow model. The

Journal of Hydraulic Engineering. Submitted July 12, 2010; accepted June 13, 2011;
posted ahead of print June 15, 2011. doi:10.1061/(ASCE)HY.1943-7900.0000474

principle assumption is that of kinematic flow.

The saturated thickness at the center of a boundary cell may be estimated by applying the method of characteristics (MOC) to the PDE for one-dimensional flow under kinematic conditions. The MOC is a mathematical solution technique for PDEs of first-order and for hyperbolic PDEs of second-order (Street, 1973). The concept of kinematic flow refers to the case where pressure and acceleration are neglected in the momentum equation (Charbeneau, 2000).

The continuity equation for 1D flow in a porous medium under unsteady conditions and with a free surface is

$$n_e \frac{\partial h}{\partial t} + \frac{\partial}{\partial x}(q * h) = r \tag{24}$$

where n_e is the effective porosity, h is the saturated thickness, r is the rainfall rate and the Darcy velocity is

$$q = -K\frac{\partial H}{\partial x} = -K\frac{\partial H}{\partial x} - KS_0 \tag{25}$$

Making this substitution and expanding the terms gives

$$n_e \frac{\partial h}{\partial t} - Kh\frac{\partial^2 h}{\partial x^2} - K\left(\frac{\partial h}{\partial x}\right)^2 - KS_0\frac{\partial h}{\partial x} = r \tag{26}$$

The assumption of kinematic conditions means that the depth gradient is neglected in the Darcy velocity, which removes the higher order terms in Eq. 26 and gives

$$n_e \frac{\partial h}{\partial t} - KS_0\frac{\partial h}{\partial x} = r \tag{27}$$

Journal of Hydraulic Engineering. Submitted July 12, 2010; accepted June 13, 2011;
posted ahead of print June 15, 2011. doi:10.1061/(ASCE)HY.1943-7900.0000474

Removing the higher order terms destroys the parabolic nature of the PDE. This is not a typical approximation for porous media flow; however, neglecting these terms allows the formulation of a boundary algorithm that considers the problem parameters and transitions smoothly to sheet flow conditions. The MOC formulation is

$$\frac{dt}{n_e} = \frac{dx}{-KS_0} = \frac{dh}{r} \tag{28}$$

To obtain a Dirichlet type boundary condition for the domain, we need to estimate the saturated thickness in the boundary cell at the new time level based on the solution from the previous time-step. Since the solution travels along characteristic curves, the idea is to determine how far the solution will move along a characteristic during a time-step. In this way the solution at time level n+1 is estimated by going up the characteristic by the proper distance. In other words, if A and B are points along the characteristic curve, the solution at point A and time level n can be used to find the solution at point B for time level n+1. The problem now is to find the distance from point B to point A. Integrating the second and third terms of Eq. 28 gives an estimate of the boundary value in terms of the distance up the characteristic curve

$$\frac{x_2 - x_1}{-KS_0} = \frac{h_2 - h_1}{r} \rightarrow h_2 = h_1 - \frac{r}{KS_0}(x_2 - x_1) \tag{29}$$

Integrating the first and second terms of Eq. 28 yields an estimate of the distance in terms of the time-step:

$$\frac{t_2 - t_1}{n_e} = \frac{x_2 - x_1}{-KS_0} \rightarrow \Delta x = -\frac{KS_0 \Delta t}{n_e} \tag{30}$$

Journal of Hydraulic Engineering. Submitted July 12, 2010; accepted June 13, 2011;
posted ahead of print June 15, 2011. doi:10.1061/(ASCE)HY.1943-7900.0000474

Substituting Eq. 30 into Eq. 29 gives the estimate:

$$h_2 = h_1 + \frac{r\Delta t}{n_e} \tag{31}$$

The value of h_1 is estimated as the solution at time level n a distance Δx up the drainage slope from point h_2.

The kinematic approximation implies a maximum value for the saturated thickness that is not reflected in the algorithm. At steady state there is no change with time, so $\Delta t = 0$, which makes $\Delta x = 0$ and puts h_1 and h_2 at the same location. Since the hydraulic gradient was approximated as the pavement slope, the Darcy velocity is constant (see Eq. 25) and the saturated thickness is determined by the flow rate per unit width. For the one dimensional case, the steady state flow rate per unit width is given by the rainfall rate, r, and length of the drainage path, L.

$$h_{ss} = \frac{rL}{KS_0} \tag{32}$$

When the kinematic condition is applied to a 1D problem, the boundary is the edge of pavement and the approximation gives a maximum depth as just described. A 2D problem has boundaries at both the edge of pavement and the ends of the domain, where the road continues beyond the modeled area. The kinematic boundary condition can also be applied at the end of the domain, but the boundary values—having neglected the depth gradient in Darcy's law—will be inconsistent with the domain interior. This inconsistency results in a boundary effect. The model domain should be expanded to remove this effect from the area of interest. One approach is to ensure the

Journal of Hydraulic Engineering. Submitted July 12, 2010; accepted June 13, 2011;
posted ahead of print June 15, 2011. doi:10.1061/(ASCE)HY.1943-7900.0000474

drainage path for a water particle starting at the boundary exits the model domain rather than entering the area of interest, thereby washing out the error. The required distance is found from the longitudinal and cross slopes and the width of the pavement.

Effect on Steady State Solution

The steady state solution for 1D drainage in PFC is given by an ODE and an initial point along the solution curve is needed to integrate the equation (Charbeneau and Barrett, 2008). The kinematic approximation described above is one approach to specifying such an initial point based on the problem parameters. Figure 3 shows that the shape of the solution curve, especially near the boundary, depends upon the value that was specified at the boundary (hL). The solution curves show that the kinematic approximation does not allow the solution to draw down near the boundary as is usual near a seepage face (Simpson et al., 2003). This draw down decreases the saturated thickness but increases the hydraulic gradient; it is required because the phreatic surface must be tangent to the seepage face (Bear, 1972). In contrast, the approximation over-estimates the saturated thickness and reduces the hydraulic gradient. Which of the curves is closest to the true physical solution is unknown, but a range of possible solutions has now been established.

In Figure 3, the solutions collapse to a single curve away from the downstream boundary, but this behavior depends on the problem parameters.

Journal of Hydraulic Engineering. Submitted July 12, 2010; accepted June 13, 2011;
posted ahead of print June 15, 2011. doi:10.1061/(ASCE)HY.1943-7900.0000474

Doubling the rainfall rate for example pushes the point at which the curves collapse to the left, provided that the thickness of the PFC layer is sufficient to contain the additional flow (Figure 4). If the PFC thickness is 5cm, then doubling the rainfall rate to 1cm/hr causes sheet flow and the boundary condition for the region of PFC flow is given by the pavement thickness (Eck et al., 2011). In general, a finite pavement thickness means that the uncertainty in the boundary value matters most for low rainfall rates.

Together, these examples illustrate that the predicted value of the saturated thickness depends on the boundary value; that the boundary value is unknown only for low rainfall rates; and that the solution is less sensitive to the boundary value in this case.

Model Validation

The model formulation was validated by demonstrating that results from Perfcode agree with steady state solutions obtained analytically. The section selected for testing is 10m wide and 20m long with a 3% cross slope and 0% longitudinal slope. Other parameters were hydraulic conductivity (1cm/s), porosity (0.2), and rainfall rate (1cm/hr). Using Eq. 11 with $d = 1cm$ and $\nu = 0.01cm^2/s$, $Re = 3$, which suggests that Darcy's law applies. The mean grain diameter of 1cm represents the weighted average sieve size in the specification for PFC used by the Texas Department of Transportation (TxDOT 2004). Simulations for three conditions were performed by varying the PFC thickness: (1) PFC flow only, (2) sheet flow only, and (3) combined

Journal of Hydraulic Engineering. Submitted July 12, 2010; accepted June 13, 2011;
posted ahead of print June 15, 2011. doi:10.1061/(ASCE)HY.1943-7900.0000474

PFC and sheet flow. A plan view of the model domain for the test section (Figure 5) shows elevation contours and boundary conditions imposed on the model. Because the objective of these simulations was a comparison with analytical solutions, the domain and boundary conditions were chosen to make the flow one-dimensional. For each simulation the discharge from the outflow boundary was tracked through time. Results presented here include the drainage profile for the combined PFC/sheet flow case and runoff hydrographs from all three cases.

Modeled values of the saturated thickness and sheet flow depth along the drainage path agreed closely with the analytical solution (Figure 6). In the figure, the normalized width variable η is plotted on the abscissa. A value of $\eta = 1$ corresponds to the no flow boundary at the edge of pavement and a value of $\eta = 0$ corresponds to the kinematic drainage boundary at the edge of pavement. The scale on the figure has been plotted in reverse order so that drainage occurs from left to right. Outflow hydrographs are plotted on a logarithmic scale on account of the wide range of times required to reach steady state (Figure 7). Several points of interest are noted on the hydrographs:

- The presence of a PFC layer delays the initial discharge from the roadway, in this case by about 1 minute from when rainfall begins.
- PFC delays the peak flow by nearly 10,000 seconds—much longer than most actual storms.
- For the combined case, the transition to sheet flow is evidenced as a

Journal of Hydraulic Engineering. Submitted July 12, 2010; accepted June 13, 2011;
posted ahead of print June 15, 2011. doi:10.1061/(ASCE)HY.1943-7900.0000474

sharp increase in the slope of the hydrograph.

- For the PFC flow only, the break in slope around 8000s corresponds to the time when the outflow boundary reaches the maximum depth allowed by the kinematic condition.

Collectively, the validation results show that the depths predicted by Perfcode are consistent with the steady state equations and that the model has good mass balance properties.

Comparison with Field Data

This section compares model results with field data from a monitoring site constructed on Loop 360 near Austin, Texas. In the autumn of 2006 equipment for automatic sample collection and hydrograph measurement was installed. A drainage system was constructed using 10cm PVC pipe to collect runoff from an 18m length of roadway and direct it to the sampler. A 15cm H-flume was used to measure the flow rate from the drainage pipe. An ISCO 4230 bubbler flow meter measured the water depth in the H-flume and calculated the flow rate. An ISCO 674 tipping bucket rain gage recorded rainfall. Both rainfall and runoff were recorded in five-minute intervals, rainfall as the total depth and runoff as the average flow rate. The model application uses the measured rainfall as a model input and computes the runoff hydrograph for comparison with the measured one.

At the location of the monitoring site, Loop 360 is a four-lane divided

Journal of Hydraulic Engineering. Submitted July 12, 2010; accepted June 13, 2011;
posted ahead of print June 15, 2011. doi:10.1061/(ASCE)HY.1943-7900.0000474

highway. The monitoring site is situated on the right-hand shoulder of the south-bound traffic lanes. The traffic lanes (7.3m) and right hand shoulder (3m) slope to the drivers right-hand side at cross-slopes of 2% and 4%, respectively. The left shoulder (1.8m) drains to the left at a cross-slope of 4%. The entire section has a longitudinal slope of 2.3%. Using Eq. 11 with $d = 1cm$ and $\nu = 0.01cm^2/s$, $Re = 9$ applies to the traffic lanes, suggesting that Darcy's law gives a reasonable approximation even though some inertial effects may be present. As in the validation case, $d = 1cm$ represents the weighted average sieve size in the specification for PFC used by the Texas Department of Transportation. (TxDOT 2004). The roadway geometry for Loop 360 was used to develop input files for the model. The model domain was extended beyond the 18m length monitored so that errors in the kinematic condition on the east and west boundaries would not influence the solution in the domain of interest (Figure 8).

The storm event of July 20, 2007 was selected for simulation because it was large enough to cause substantial sheet flow and because the monitoring results had good mass balance properties. The hydraulic conductivity and porosity for this simulation correspond to values measured by Klenzendorf (2010) for a nearby location on the same highway. Values of Mannings n have not been measured for PFC, but a value of 0.015 appears appropriate considering the analysis of Charbeneau et al. (2009).

During the storm of July 20, 2007 the monitoring site received 48mm of rainfall over a 5.6 hour period. The peak rainfall depths on a five, fifteen and sixty minute intervals were 6.6mm, 18mm, and 39mm, respectively. On

Journal of Hydraulic Engineering. Submitted July 12, 2010; accepted June 13, 2011;
posted ahead of print June 15, 2011. doi:10.1061/(ASCE)HY.1943-7900.0000474

a sixty minute basis, the storm corresponded to a return period of about 2 years (Asquith and Roussel 2004).

A model time step of 5s was used when the all of the drainage was contained within the pavement, but a step of 0.1s was needed during sheet flow for the model to remain stable. In order to make a fair comparison with the field measurements, the calculated flow rates were averaged over five minute intervals. A weighted average flow rate was used so that a five-minute interval containing two sizes of time step had the proper flow rate. These averaged flow rates showed generally good agreement with the field measurements (Figure 9). The model predicted peak flows of the proper time and magnitude, and the shape of the hydrograph generally matches the field observations.

The model predicted a peak flow 3.7 L/s, which is 97% of the measured value of 3.8 L/s. The difference between the modeled and measured flow rates (residual) had a mean –0.029L/s, median 0.021 L/s, standard deviation 0.24 L/s and standard error of the mean 0.029 L/s. The largest residuals were associated with high flow rates. This comparison suggests that the model parameters were consistent with field conditions and lends credibility to the associated depth predictions.

During this simulation, maximum depth in the domain of interest was 5.142cm above the impervious layer, which represents a sheet flow depth of 1.4mm. This maximum occurred near the edge of the right traffic lane (Figure 10). The exact location was 3.2m from the southern edge of the domain; since the shoulder width is 3.05m, the maximum depth occurred

Journal of Hydraulic Engineering. Submitted July 12, 2010; accepted June 13, 2011;
posted ahead of print June 15, 2011. doi:10.1061/(ASCE)HY.1943-7900.0000474

15cm from the shoulder. This peak occurred 1 hour after rainfall began (3599.9s) and during the peak rainfall intensity of 80 mm/hr. Model results further showed that sheet flow depths in excess of 0.1mm persisted for 1600 seconds during this event, but would have persisted for 8580 seconds without the PFC layer. This difference represents a reduction of 81% in the duration of sheet flow conditions.

The model results show that sheet flow begins 1.6m due south of the grade break for the left hand shoulder (Figure 10). Under most conditions, this break in slope acts as a no-flow boundary within the domain; the no flow condition is assumed here for purposes of comparison with the analytical model even though some flow does occur. At the peak rainfall rate for this storm, the analytical model (see Charbeneau and Barrett, 2008 and Eck et al., 2011) predicts sheet flow at 2m down the drainage slope or 1.4m due south of the grade break. This location differs from Perfcode's estimate by 20cm, which seems a reasonable match considering that the numerical model is not at steady state and that the boundary condition is approximate.

A comparison between model results and field measurements was made for a second storm event to confirm that the results obtained for July 20, 2007 were not coincidental. During the storm of November 24, 2007 the monitoring site received 25mm of rainfall over a 28 hour period ,which is much less rainfall than a 2-year 24 hour storm (86mm, Asquith and Roussell 2004). The peak rainfall depths on five, fifteen and sixty minute intervals were 1.3mm, 2.0mm, and 4.1mm. According to the cumulative rainfall intensity curve given by Charbeneau and Barrett (2008), approximately 75% of Austin's

Journal of Hydraulic Engineering. Submitted July 12, 2010; accepted June 13, 2011;
posted ahead of print June 15, 2011. doi:10.1061/(ASCE)HY.1943-7900.0000474

rainfall occurs at or below the intensity of 4mm/hr. These peak rainfall depths are less than 20% of the values for the July 20 storm, illustrating that the November 24 event represents different hydrological conditions. The measured rainfall data was prepared for simulation as outlined previously; all other simulation parameters remained the same.

The modeled hydrograph again shows reasonable agreement with the measured one (Figure 11). The model predicted a peak discharge of 0.26 L/s, which matches the measured peak discharge of 0.26 L/s. Statistics of the residuals had a mean 5.7e-7 L/s, median -0.0063 L/s, standard deviation 0.023 L/s, and standard error of the mean 0.0028 L/s. As seen in Figure 11, the H-flume used for monitoring has difficulty distinguishing flow rates near zero (0.01 L/s). During this storm the maximum depth within the PFC layer was 1.5cm so the PFC layer prevented sheet flow conditions entirely. This comparison confirms that Perfcode gives robust results for a range of hydrological conditions. Further details in model development and testing are presented by Eck (2010).

Conclusions

The development, validation and application of Perfcode has provided insight into the drainage behavior of PFC highways. The kinematic boundary condition developed for PFC flow addresses an important gap in the literature of porous pavement hydraulics: the depth at the boundary can now be estimated for steady state or transient conditions. At the edge of pavement this

Journal of Hydraulic Engineering. Submitted July 12, 2010; accepted June 13, 2011;
posted ahead of print June 15, 2011. doi:10.1061/(ASCE)HY.1943-7900.0000474

condition gives a maximum depth in the PFC layer; but at the ends of the domain depth estimates are inconsistent with the domain interior, resulting in a boundary effect. The model domain should therefore be expanded to remove this effect from the area of interest. Use of this boundary condition yielded hydrographs that were consistent with field measurements.

Predictions of runoff hydrographs for PFC roadways are available for the first time. These hydrographs show that PFC delays the initial discharge from the roadway compared to conventional pavement and that flow in a PFC layer requires a long time to reach steady state. For a constant rainfall case, PFC delayed the initial discharge by 60 seconds and required 50 times more rainfall to reach steady state, though these values depend on problem parameters.

One dimensional steady state equations remain a powerful tool for engineering design. For the storm investigated, the 1D steady state equations predicted the location that sheet flow begins within 20cm of Perfcode's prediction. The location and magnitude of the maximum sheet flow depth were also closely predicted by the 1D steady state equations. This result confirms that the steady state equations are suitable for aiding design of PFC thickness on straight roads, though such models cannot address roadways with spatially variable configuration nor the dynamic response of roadway drainage.

Perfcode is applicable to a variety of practical problems related to PFC highways. Applications include selection of PFC layer thickness for a design event, comparisons of drainage performance with and without a PFC layer

Journal of Hydraulic Engineering. Submitted July 12, 2010; accepted June 13, 2011;
posted ahead of print June 15, 2011. doi:10.1061/(ASCE)HY.1943-7900.0000474

and analysis of more complex roadway geometry such as sag vertical curves and superelevation transitions. Future work will examine these areas and the effect of curb and gutter edge treatments on the drainage performance of PFC roadways.

Acknowledgements

The authors gratefully acknowledge the research support provided by the Texas Department of Transportation through the Center for Transportation Research at The University of Texas at Austin. We especially thank Gary Lantrip of TxDOT for his interest in PFC research.

Notation

The following symbols are used in this paper:

A = area [L^2];
b = thickness of PFC layer [L];
C = conveyance coefficient [1/T];
$D(h_s)$ = non-linear diffusion coefficient for sheet flow [$L^{5/3}$];
d = mean grain diameter [L];
H = piezometric head [L];
h_p = thickness of water in the PFC layer [L];
h_s = thickness of water on the PFC surface [L];
K = hydraulic conductivity [L/T];
ℓ = length of a curvilinear segment [L];

Journal of Hydraulic Engineering. Submitted July 12, 2010; accepted June 13, 2011;
posted ahead of print June 15, 2011. doi:10.1061/(ASCE)HY.1943-7900.0000474

N = number of elements [–];

n = Manning coefficient [–];

$\hat{n}$ = unit normal vector;

n_e = effective porosity [–];

pf = porosity function [–];

Q = volumetric flow rate [L^3/T];

$\vec{q}$ = specific discharge [L/T];

r = rainfall rate [L/T];

S_f = friction slope [–];

S_0 = pavement slope [–];

$\vec{v}$ = velocity of sheet flow [L/T];

x = horizontal coordinate distance [L];

y = horizontal coordinate distance [L];

z = elevation of the bottom of the PFC layer;

η = transverse curvilinear coordinate [–];

ω = width of curvilinear segment [–];

ξ = longitudinal curvilinear coordinate [–];

References

Asquith, W.H., and Roussel, M.C., 2004, Atlas of depth-duration frequency of precipitation annual maxima for Texas: U.S. Geological Survey Scientific Investigations Report 20045041, 106 p.

Journal of Hydraulic Engineering. Submitted July 12, 2010; accepted June 13, 2011;
posted ahead of print June 15, 2011. doi:10.1061/(ASCE)HY.1943-7900.0000474

Barrett, Michael E. (2008), Effects of a Permeable Friction Course on Highway Runoff, Journal of Irrigation and Drainage Engineering, Vol. 134, No. 5.

Bear, Jacob. (1972), Dynamics of Fluids in Porous Media, Elsevier, New York.

Charbeneau, Randall J. (2000), Groundwater Hydraulics and Pollutant Transport, Waveland Press, Long Grove, IL.

Charbeneau, Randall J. and Barrett, Michael E. (2008), Drainage Hydraulics of Permeable Friction Courses, Water Resources Research 44, W04417.

Charbeneau, Randall J., Jeong, Jaehak, and Barrett, Michael E. (2009). Physical Modeling of Sheet flow on Rough Impervious Surfaces, Journal of Hydraulic Engineering, Vol 135. No. 6.

Eck, Bradley J. (2010) Drainage Hydraulics of Porous Pavement: Coupling Surface and Subsurface Flow. Dissertation. The University of Texas at Austin.

Eck, Bradley J., Barrett, Michael E., Charbeneau, Randall J. (2011). Correction to Drainage hydraulics of permeable friction courses Water Resources Research doi:10.1029/2010WR009877 (in press)

Daluz Vieira, J.H. (1983), Conditions Governing the Use of Approximations for the Saint-Venant Equations for Shallow Surface Water Flow. Journal of Hydrology, 60: 43-58.

Ferziger, Joel H. and Peric, Milovan. (2002), Computational Methods for Fluid Dynamics, Springer, Berlin.

Furman, Alex. (2008), Modeling Coupled Surface-Subsurface Flow Pro-

Journal of Hydraulic Engineering. Submitted July 12, 2010; accepted June 13, 2011;
posted ahead of print June 15, 2011. doi:10.1061/(ASCE)HY.1943-7900.0000474

cesses: A Review. Vadose Zone Journal, 7:741-756.

Halek, Vaclav and Svec, Jan. (1979), Groundwater Hydraulics. Elsevier, New York.

He, Zhiguo, Wu, Weiming, and Wang, Sam S. Y. (2008), Coupled Finite-Volume Model for 2D Surface and 3D Subsurface Flows. Journal of Hydrologic Engineering, Vol. 13 No. 9.

Jeong, Jaehak and Charbeneau, Randall J. (2010), Diffusion Wave Model for Simulating Storm-water Runoff on Highway Pavement Surfaces at Superelevation Transition, Journal of Hydraulic Engineering, 136, 770.

Klenzendorf, Joshua B. (2010), Hydraulic Conductivity Measurement of Permeable Friction Course (PFC) Experiencing Two-Dimensional Nonlinear Flow Effects. Dissertation. University of Texas at Austin.

Liang, Dongfang, Falconer, Roger A., and Lin, Binliang. (2007), Coupling surface and subsurface flows in a depth averaged flood wave model. Journal of Hydrology, 337:147-158.

NCHRP: National Cooperative Highway Research Program (2009), Construction and Maintenance Practices for Permeable Friction Courses, Report 640, Transportation Research Board, Washington, D.C..

Ranieri, Vittorio. (2002), Runoff Control in Porous Pavements, Transportation Research Record.1789, pp.46-55.

Refsgaard, Jens Christian and Storm, Borge. (1995), MIKE-SHE. p. 809846. In V.P. Singh (ed.) Computer models of watershed hydrology. Water Resour. Publ., Highlands Ranch, CO.

Simpson, M.J., Clement, T.P. and Gallop, T.A. (2003), Laboratory and

Journal of Hydraulic Engineering. Submitted July 12, 2010; accepted June 13, 2011;
posted ahead of print June 15, 2011. doi:10.1061/(ASCE)HY.1943-7900.0000474

Numerical Investigation of Flow and Transport Near a Seepage-Face Boundary. Ground water. Vol. 41 No.5 pp690-700.

Street, Robert L. (1973), The Analysis and Solution of Partial Differential Equations, Brooks/Cole, Monterey, California.

Tan, S.A., T.F. Fwa, and K.C. Chai (2004), Drainage consideration for Porous Asphalt Surface Course Design, in Transportation Research Record 1868, pp 142-149.

Texas Department of Transportation (TxDOT), (2004) "Standard specifications for construction and maintenance of highways, streets, and bridges." Item No. 342, 312-329, URL: http://www.dot.state.tx.us/business/ specifications.htm Mar. 20, 2005.

Journal of Hydraulic Engineering. Submitted July 12, 2010; accepted June 13, 2011;
posted ahead of print June 15, 2011. doi:10.1061/(ASCE)HY.1943-7900.0000474

Figure Captions

Figure 1: Schematic cross section of permeable friction course roadway

Figure 2: Curvilinear grid generation scheme for highway drainage modeling

Figure 3: Steady state drainage profile for different boundary values; all cases used K=1cm/s, S_0=3%; r=0.5cm/hr

Figure 4: Steady state drainage profile for different boundary values; all cases used K=1cm/s, S_0=3%; r=1cm/hr

Figure 5: Plan view of model validation domain showing elevation contours and boundary conditions

Figure 6: Comparison of Perfcode with analytical solution for steady state drainage from a 5cm PFC layer. Model parameters were drainage slope (3%), length (10m), rainfall rate (1cm/hr), hydraulic conductivity (1cm/s) and porosity (0.2)

Figure 7: Runoff hydrographs from a linear section

Figure 8: Simulation domain for Loop 360 monitoring site showing elevation contours (m)

Figure 9: Comparison of modeled and measured hydrographs for storm of July 20, 2007

Journal of Hydraulic Engineering. Submitted July 12, 2010; accepted June 13, 2011;
posted ahead of print June 15, 2011. doi:10.1061/(ASCE)HY.1943-7900.0000474

Figure 10: Profile through maximum depth section for July 24, 2007; the horizontal coordinate is 94.42m on Figure 8

Figure 11: Comparison of modeled and measured hydrographs for storm of November 24, 2007

Figure 1

Journal of Hydraulic Engineering. Submitted July 12, 2010; accepted June 13, 2011;
posted ahead of print June 15, 2011. doi:10.1061/(ASCE)HY.1943-7900.0000474

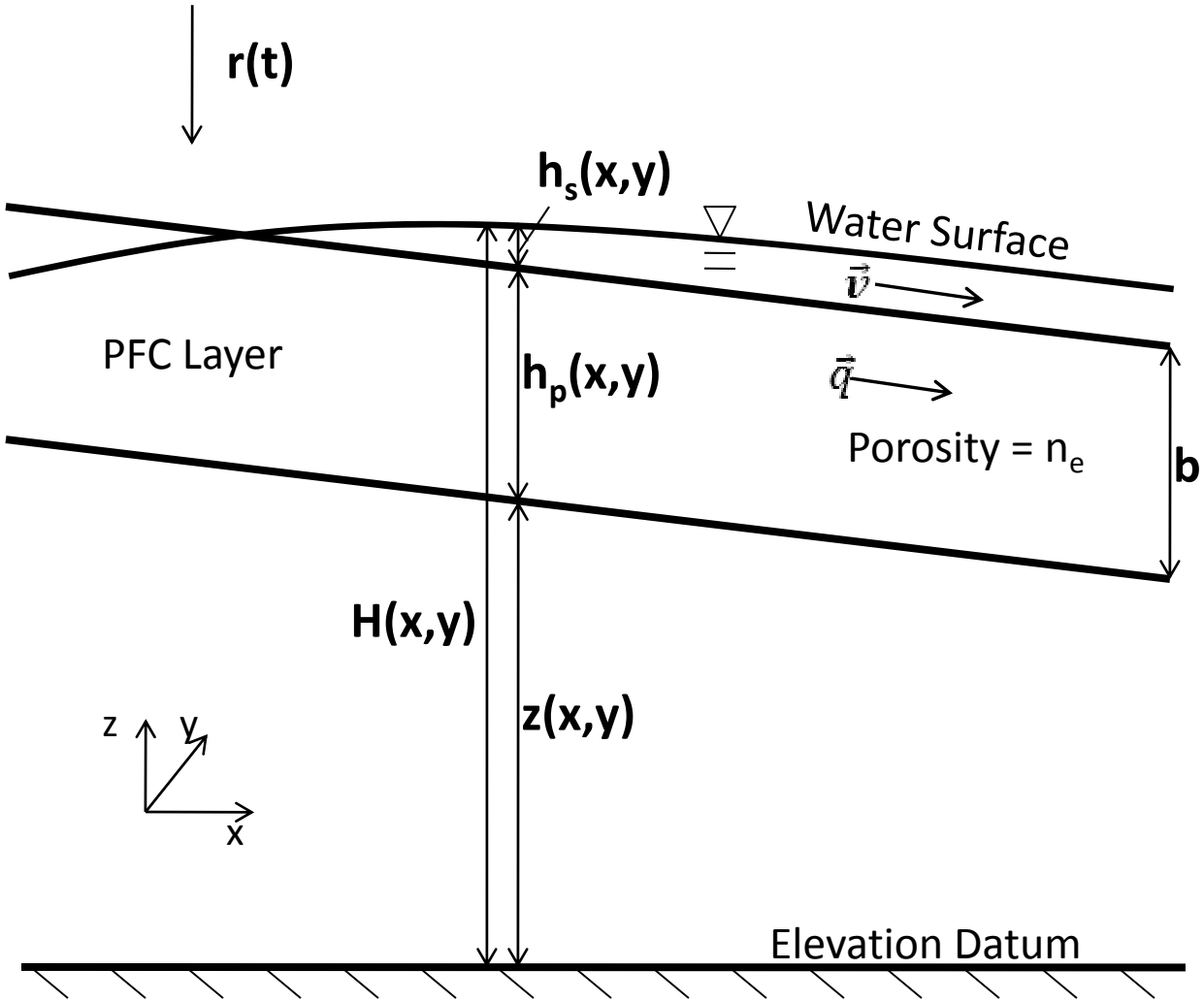

Figure 1: Schematic cross section of permeable friction course roadway

Figure 2

Journal of Hydraulic Engineering. Submitted July 12, 2010; accepted June 13, 2011;
posted ahead of print June 15, 2011. doi:10.1061/(ASCE)HY.1943-7900.0000474

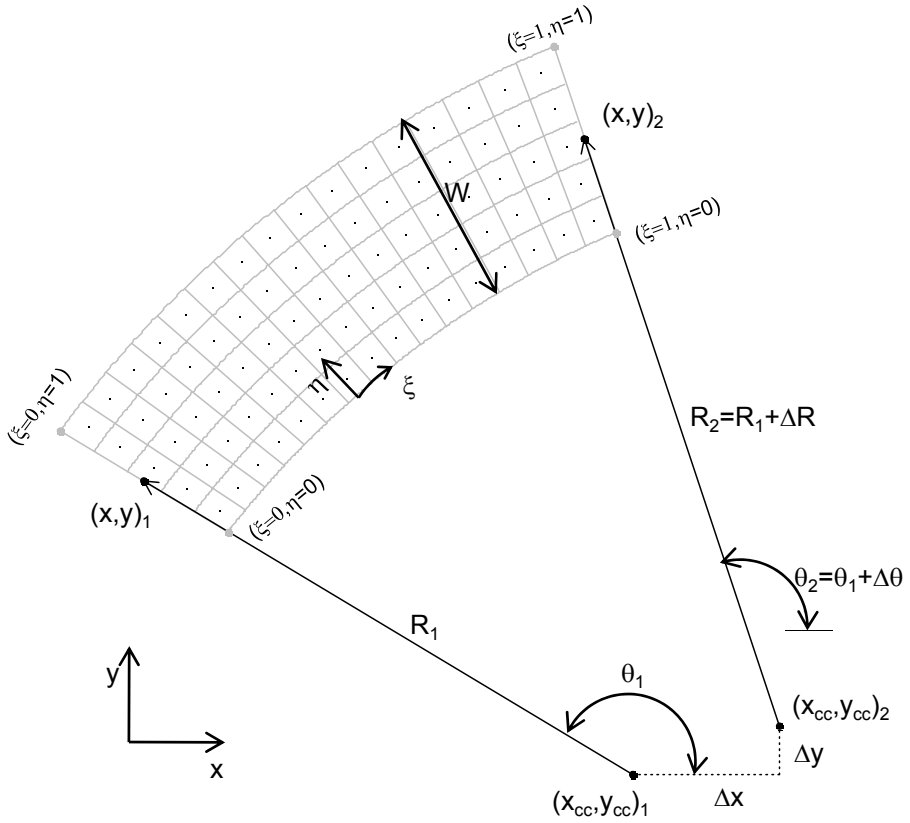

Figure 2: Curvilinear grid generation scheme for highway drainage modeling

Figure 3

Journal of Hydraulic Engineering. Submitted July 12, 2010; accepted June 13, 2011;
posted ahead of print June 15, 2011. doi:10.1061/(ASCE)HY.1943-7900.0000474

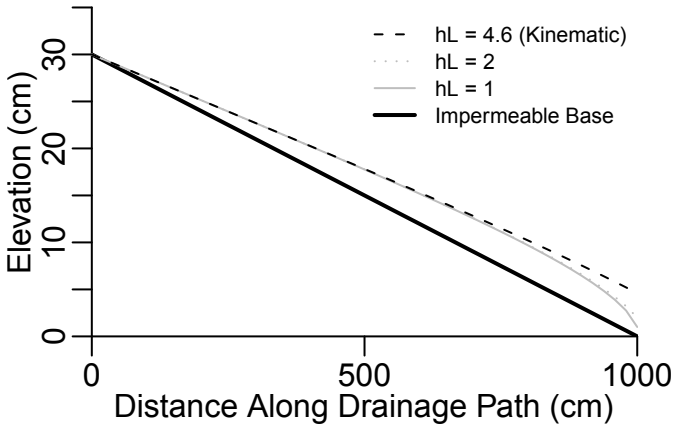

Figure 3: Steady state drainage profile for different boundary values; all cases used K=1cm/s, S_0=3%; r=0.5cm/hr

Figure 4

Journal of Hydraulic Engineering. Submitted July 12, 2010; accepted June 13, 2011;
posted ahead of print June 15, 2011. doi:10.1061/(ASCE)HY.1943-7900.0000474

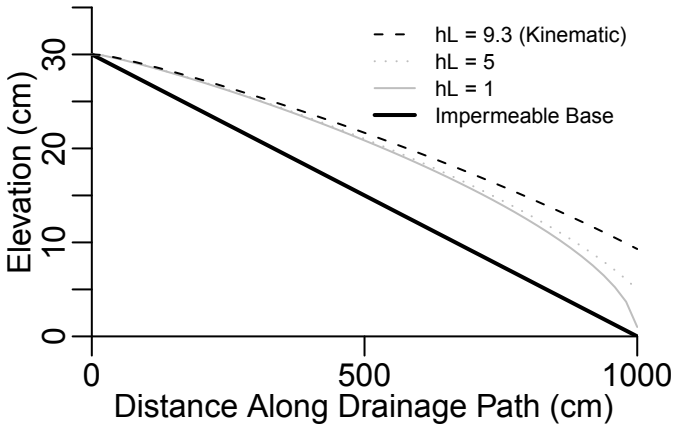

Figure 4: Steady state drainage profile for different boundary values; all cases used K=1cm/s, S_0=3%; r=1cm/hr

Figure 5

Journal of Hydraulic Engineering. Submitted July 12, 2010; accepted June 13, 2011;
posted ahead of print June 15, 2011. doi:10.1061/(ASCE)HY.1943-7900.0000474

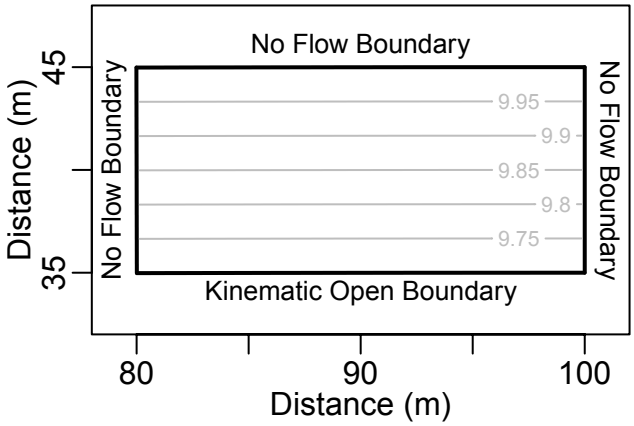

Figure 5: Plan view of model validation domain showing elevation contours and boundary conditions

Figure 6

Journal of Hydraulic Engineering. Submitted July 12, 2010; accepted June 13, 2011;
posted ahead of print June 15, 2011. doi:10.1061/(ASCE)HY.1943-7900.0000474

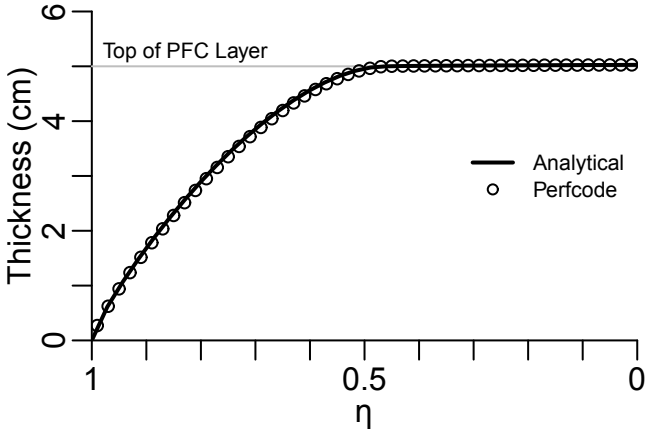

Figure 6: Comparison of Perfcode with analytical solution for steady state drainage from a 5cm PFC layer. Model parameters were drainage slope (3%), length (10m), rainfall rate (1cm/hr), hydraulic conductivity (1cm/s) and porosity (0.2)

Figure 7

Journal of Hydraulic Engineering. Submitted July 12, 2010; accepted June 13, 2011;
posted ahead of print June 15, 2011. doi:10.1061/(ASCE)HY.1943-7900.0000474

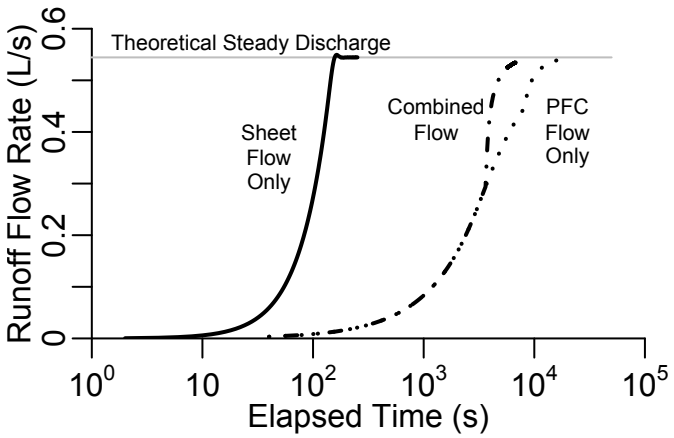

Figure 7: Runoff hydrographs from a linear section

Figure 8

Journal of Hydraulic Engineering. Submitted July 12, 2010; accepted June 13, 2011;
posted ahead of print June 15, 2011. doi:10.1061/(ASCE)HY.1943-7900.0000474

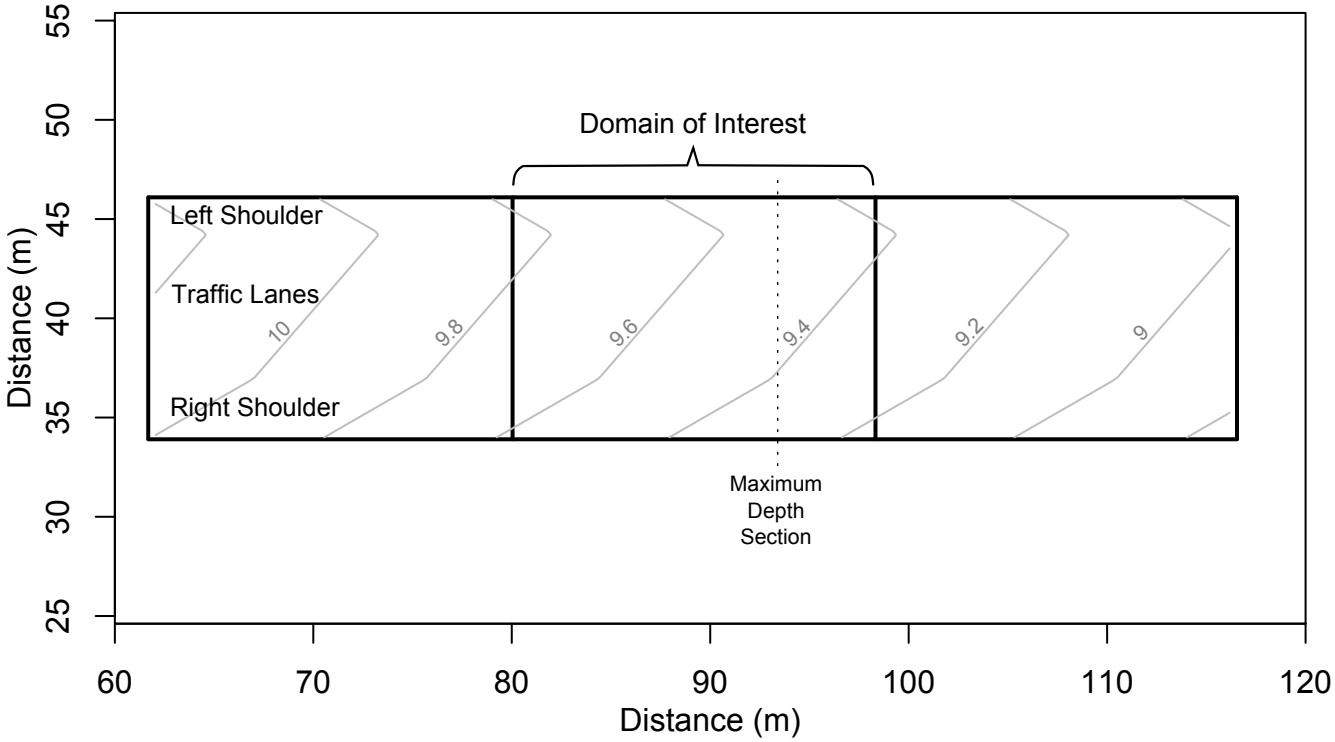

Figure 8: Simulation domain for Loop 360 monitoring site showing elevation contours (m)

Figure 9

Journal of Hydraulic Engineering. Submitted July 12, 2010; accepted June 13, 2011;
posted ahead of print June 15, 2011. doi:10.1061/(ASCE)HY.1943-7900.0000474

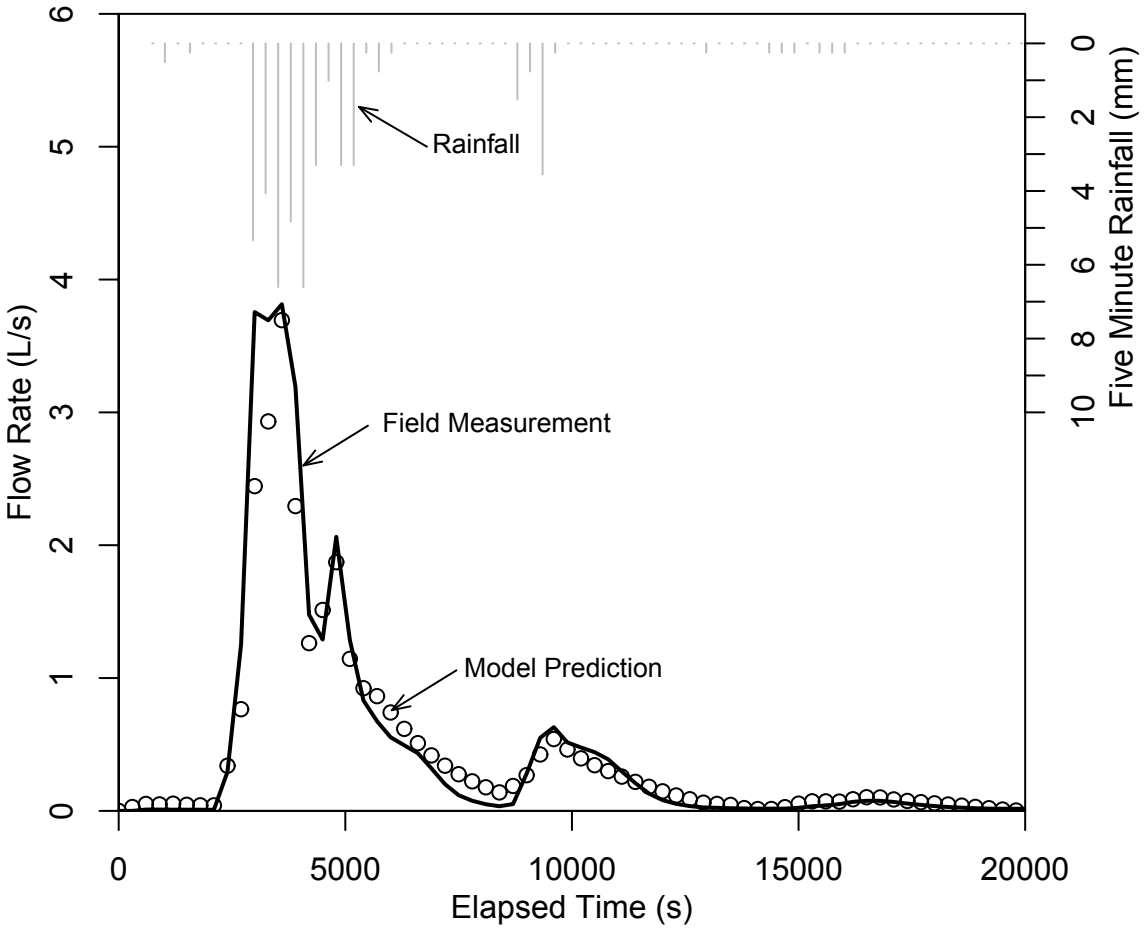

Figure 9: Comparison of modeled and measured hydrographs for storm of July 20, 2007

Figure 10

Journal of Hydraulic Engineering. Submitted July 12, 2010; accepted June 13, 2011;
posted ahead of print June 15, 2011. doi:10.1061/(ASCE)HY.1943-7900.0000474

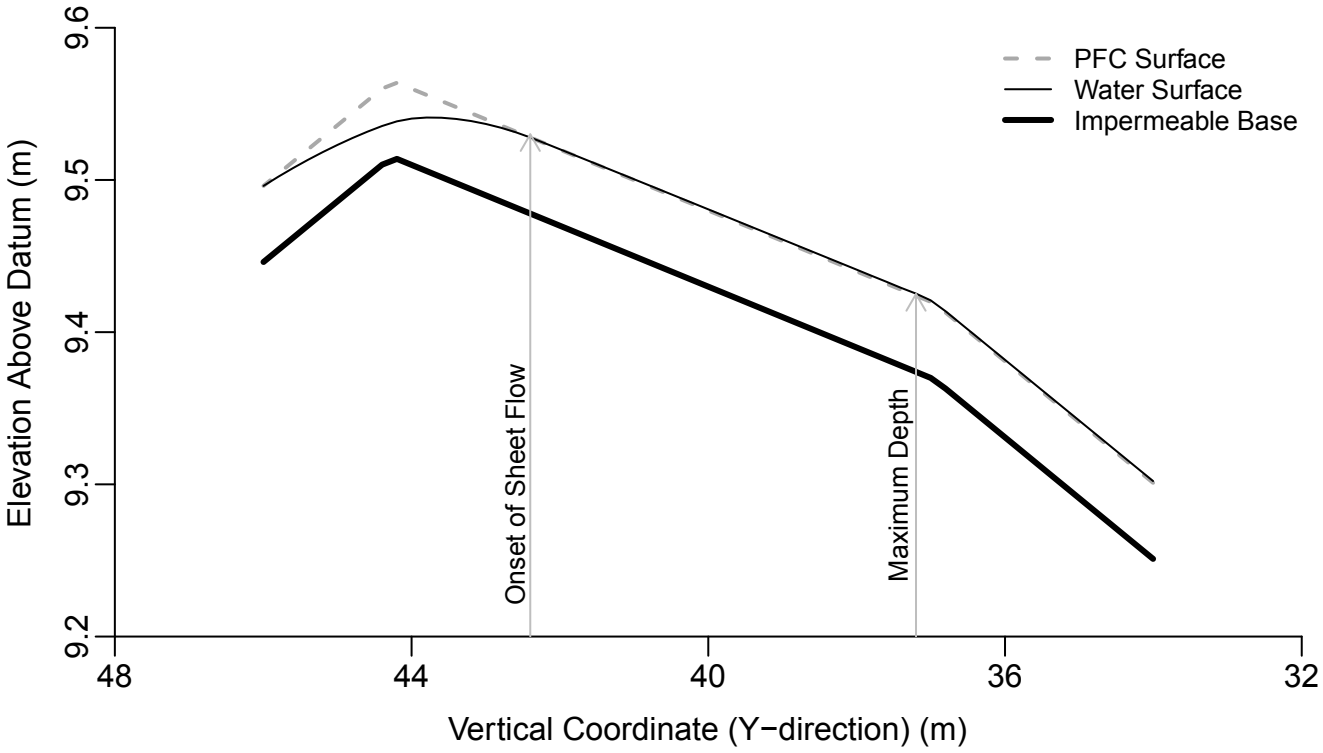

Figure 10: Profile through maximum depth section for July 24, 2007; the horizontal coordinate is 94.42m on Figure 8

Figure 11

Journal of Hydraulic Engineering. Submitted July 12, 2010; accepted June 13, 2011;
posted ahead of print June 15, 2011. doi:10.1061/(ASCE)HY.1943-7900.0000474

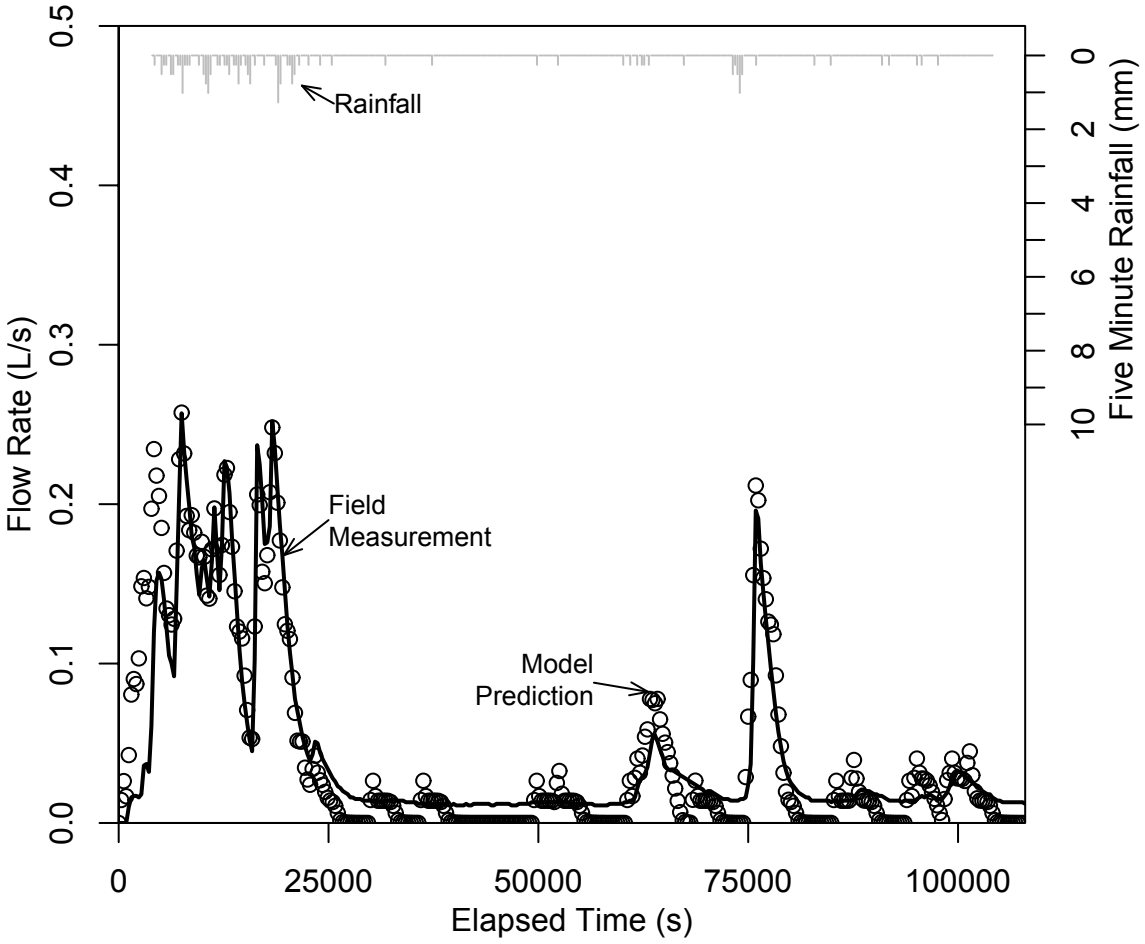

Figure 11: Comparison of modeled and measured hydrographs for storm of November 24, 2007